To appear in Proceedings of the Symposium on Developments in Fluid Dynamics and Aerospace Engineering, Bangalore, India, December 9–10, 1993.

FREE SHEAR LAYERS, BASE PRESSURE AND BLUFF-BODY DRAG

A. Roshko
Graduate Aeronautical Laboratories
California Institute of Technology
Pasadena, CA, U.S.A. 91125

ABSTRACT

Incompressible, non-vortex-shedding bluff-body flows and supersonic base-pressure flows are discussed from a unified viewpoint in which the aspect ratio of the near wake is determined from the balance of shear-stress and pressure forces on the near-wake boundary. The base pressure and drag are then determined from free-streamline theory. The analysis is incomplete, for want of sufficient information about conditions in reattaching supersonic turbulent shear layers.

1. INTRODUCTION

The problem of bluff-body drag at high Reynolds number is one of the oldest unsettled ones in fluid dynamics. Leonardo's famous sketches depict flow around cylindrical structures and his notebooks contain references to the "force of the flow". Newton obtained a formula for the force on a flat plate of area A set normal to a flow which he represented by a stream of particles (Fig. 1a), having momentum flux per unit area mNU^2 ($= \rho U^2$ in fluid flow notation). Assuming that the plate absorbs all this momentum the drag force is $D = \rho U^2 A$ which gives a value of drag coefficient, $C_D \equiv D/\frac{1}{2}\rho U^2 A = 2$. While this value is indeed close to measured values of drag of such bluff plates with large span, the flow field and pressure distribution in a continuum fluid are rather different from those in Newton's model, especially in subsonic flow. For a disc the model would give the same value, $C_D = 2$, but the actual drag coefficient in incompressible flow is $C_D = 1.1$.

The modern era of bluff-body modelling began with the mathematical paper of Kirchhoff [1], who used the free-streamline method of Helmholtz to represent the flow past the bluff flat plate (Fig. 1b). This captures many of the important features of bluff-body flow: (i) separation, here from the edges of the plate; (ii) the resulting free shear layers, represented as the surfaces of velocity discontinuity, $\psi = 0$; (iii) a low value of "base-pressure" coefficient, having in this case a value which is *set* at $C_{p_b} = 0$; and (iv) a correspondingly high value of drag coefficient, in this case 0.88, made up entirely of *pressure drag*, but only about half the value actually observed in real flow past a flat plate. The discrepancy is related to an important feature, missing in Kirchhoff's flow, namely the near-wake "closure" or "reattachment" of the free shear layers. Kirchhoff's wake is open to downstream infinity whereas real wakes tend to close by the action of laminar or turbulent diffusion. An extreme case of such diffusion occurs when the

separated shear layers roll up soon after separation, alternately forming and "shedding" vortices on each side of the wake. Wake closure results in $C_{p_b} < 0$ and C_D correspondingly higher, the actual values depending on the situation. For example, a splitter plate placed on the centerplane downstream of the body eliminates the vortex shedding instability; the closure is then effected mainly by turbulent diffusion of the free shear layers, located around $\psi = 0$. The drag is then not as high as with vortex shedding but still higher than Kirchhoff's value.

The Kirchhoff model for the wake is for steady flow; its possible application to real, unsteady (vortex-shedding, turbulent) flows requires that a correspondence be sought between mean values of drag (C_D), pressure coefficients (C_p), etc. and the *mean flow*. For example, the mean flow field for flow past a flat plate or "wall", of diameter d at Reynolds number $U_\infty d/\nu \equiv Re = 10^5$, is shown in Fig. 2a from Ref. 2. In the actual unsteady flow (Fig 2b) there is vigorous vortex shedding, at a frequency $fd/U_\infty = St \doteq 0.14$, as well as other turbulent fluctuation. The values [3] of base *suction* ($-C_{p_b} = 1.4$) and drag coefficient ($C_D = 2.1$) are considerably higher than those from the Kirchhoff model. When a splitter plate is placed in the near wake, the vortex shedding instability is eliminated, the mean flow is strikingly altered, as shown in Fig. 2c, and the values of base suction and drag are reduced to $-C_{p_b} = 0.6$ and $C_D = 1.4$, respectively [2]. For these mean flows an improvement over Kirchhoff's model can be obtained by adopting a different class of free-streamline models, for example the one proposed by Riabouchinsky [4] which provides for *closure* of the wake by the device of an "image body" at a distance $x = L$ from the bluff body (Fig. 1c). The wake length L and width W depend on the value of base pressure $C_{p_b} = C_{p_w}$, which now becomes a *parameter* of the problem; in fact it is the crucial parameter that must be understood and modelled in the quest for a "solution" to the bluff-body problem.

In Ref. 5 we discussed a possible model for bluff-body flows based on the idea [6] that the wake pressure is set by the balance of shear-stress and pressure forces acting on the boundary of the wake which is defined by a free-streamline model such as Riabouchinsky's. When vortex shedding is not present the instantaneous flow field is not greatly different from the mean flow; the shear stresses are maximum near the zero streamlines, while the main pressure change (a pressure rise) occurs in the closure region, which in effect replaces the Riabouchinsky image body. In Ref. 5 we did not address this region adequately; it will be the main focus of the present discussion.

The problem of pressure rise in the closure region was addressed in the famous papers of Chapman *et al.* [7] and Korst [8], principally for *supersonic base flow*. Here we attempt to present a unified view of both the supersonic base-pressure problem and the incompressible bluff-body problem without vortex shedding, first comparing the two cases for flow over a step. For supersonic flow, this easily generalizes to cases with various forebody shapes, e.g. a family of wedges, because the forebody is uncoupled from the base but the corresponding incompressible class of flows is more difficult in the sense that the whole flow field is interactive; this is discussed in the following sections.

In these flows the separated free shear layer which develops around $\psi = 0$ plays a central

role. For reference, we have summarized in the Appendix the salient properties of canonical free shear layers, for possible use in the development of the model.

2. SUPERSONIC BASE FLOW

The classic supersonic base flow is illustrated in Fig. 3. It also exhibits the typical bluff-body features: separation at the edges of the base; free shear layers at constant pressure, which is lower than that upstream of the base; corresponding base "suction" or drag. In two dimensional flow the free streamlines are straight, terminating at the closure or reattachment point, r, where the flow has to turn back into the free-stream direction to a "downstream" pressure p_d which, in two dimensional flow, is very close to p_1. Because the vortex shedding instability is absent in supersonic flow, introduction of a stabilizing barrier along the centerplane, i.e. a splitter plate in Fig. 3a has little effect other than to perturb the small backflow which may be present in the near wake and hardly changes the base pressure [9, 10]. Thus, the upper half of the base flow in Fig. 3a is little different from the flow over a backward facing step in Fig. 3b. The corresponding subsonic base flow without vortex shedding is shown in Fig 3c; it may be either flow over a step or over a base with splitter plate.

Fig. 3 contrasts the simpler free-streamline geometry for supersonic flow with the incompressible case in Fig. 1. The connection between wake pressure and wake geometry is also simpler for the supersonic case; i.e. the wake length L (Fig. 3b) is simply related to p_w by the Prandtl-Meyer expansion from p_1 to $p_w(= p_b)$. Decrease of L corresponds to decrease of p_b and increased drag. It is also clear that conditions at the reattachment point, r, must play an important role. In the free streamline model r is a point of velocity discontinuity but in the real flow it is at the termination of the zero streamline $\psi^* = 0$ which is now imbedded in the free shear layer (Fig. 4) that develops around the inviscid location $\psi = 0$. In developing a model of this flow, it is useful to consider an asymptotic condition in which the free shear layer, starting with initial thickness $\theta_0 = 0$ at separation, develops at constant pressure $p_s = p_e$ with velocity $U_s = U_e$ outside and zero velocity inside (i.e. neglecting any motion inside the so called "dead water" region). Then use can be made of data from experiments or computations on canonical free shear layers. A summary of such data is given in the Appendix.

Almost forty years ago, Chapman *et al.* [7] and Korst [8] independently proposed a criterion for closing the problem, i.e. finding the dynamically compatibile pair, p_b and L. Known as the Chapman-Korst (Ch-K) criterion (Ch for laminar flow, K for turbulent), the criterion is that the total pressure p_t^* on the reattaching streamline $\psi^* = 0$, which is embedded in the shear layer (Fig. 4), must be equal to the downstream pressure $p_d(\doteq p_1)$, to ensure that the streamlines outside $\psi^* = 0$ have sufficient energy to reach p_d without flow reversal.

The criterion seemed to work astonishingly well. For example, assuming that the initial free shear-layer thickness at separation, θ_s/h, is small enough to allow a self similar, equilibrium free shear layer to develop, values of p_b/p_1 calculated for values of M_1 between 1.5 and 4 are within a few percent of measured values [8]. For larger values of θ_s/h a higher value of base

pressure is predicted because there is not sufficient distance before reattachment (at r) for u^* and p_t^* to reach their maximum, asymptotic values; the reattachment point would move further downstream to r' to allow a higher value of wake pressure p'_w, thus a lower value of required pressure rise, $p_d - p'_w$. Success in rationalizing these and other effects on base pressure made the Ch-K criterion very attractive.

However, there were notable exceptions which, taken together with evident difficulties in the theoretical idea of Korst and Chapman, led to re-examinations of the problem, eg. Nash [11]. The difficulty on the theoretical side appears in a well-known inconsistency in the Korst-Chapman idea: recompression along the dividing streamline is supposed to be isentropic up to the point of reattachment or flow reversal (Fig. 4), that is, $p_r = p_t^*$. However there must be additional pressure rise beyond the point r, due to recovery in the upper part of the shear profile. That is, $p_d > p_r$ and so $p_d > p_t^*$, in contradiciton to the basic assumption noted above. Experiments confirm that the point of reattachment r lies only part way up the pressure rise curve, i.e. $p_r < p_d$, as sketched in Fig. 4. Chapman and Korst [12], aware of this difficulty, speculated that compensating effects must be at work to produce the pressure rise given by their formulas, namely a loss of total pressure on the dividing streamline in the "dissipative region" near reattachment, resulting in $p_r < p_t^*$, is compensated by the further rise of pressure in the development region downstream of r. But Nash cited experimental results which gave values of base pressure lower than the lowest limiting values predicted by Ch-K theory and presented an analysis which suggested that the discrepancy was in fact due to effects of initial shear-layer thickness and could be significant. His conclusions were supported in experiments by Sirieix *et al.* [13, 14]. The latter demonstrated an even more serious problem with the Ch-K criterion: they were able to modify the wall just downstream of r, thus changing the pressure distribution downstream of r, without affecting the pressure and the base flow upstream of r!

Modifications of the Ch-K criterion have been proposed, eg. by Sirieix *et al.*, and other approaches to the base-pressure problem have been explored; for example, Tanner [15] developed a "wake-outflow" concept which focusses attention on the entrainment into the free shear layers and looks for a momentum balance with the pressure forces. In the following, we explore a model in which the momentum balance is between pressure and *shear-stress* forces, as initially proposed by Sychev [6] in his attempt to develop an asymptotic ($Re \to \infty$) model for *steady, laminar* bluff-body flow. Before proceeding with supersonic base flow we return to the incompressible case, where quantitative experimental data for turbulent free shear layers is more complete (cf. the Appendix).

3. SUBSONIC BASE FLOWS

Chapman *et al.* [7] had suggested that their criterion was also relevant to nonshedding subsonic base flows, like the one sketched in Fig. 3c, for which a separated free shear layer is defined. To further explore this, Roshko and Lau [16] obtained pressure distributions in the reattachment region downstream of separation ($x = 0$) for the various nonshedding geometries shown in Fig. 5a. The difficulty in using the criterion for prediction of base pressure in subsonic

flow, because of the interactive nature of the whole flow field, is evident from the variety of pressure distributions, which provide no obvious guide for defining the downstream pressure p_d. However, a useful comparison of these distributions is obtained by rewriting them in terms of a *reduced pressure-rise coefficient* $\widetilde{C}_p \equiv (p - p_e)/\frac{1}{2}\rho U_e^2$, referenced to the dynamic pressure at the edge of the reattaching shear layer, instead of the conventional coefficient $C_p \equiv (p - p_\infty)/\frac{1}{2}\rho U_\infty^2$. Such a definition had been introduced by Crabtree [17] to correlate pressure rise in leading-edge separation bubbles on airfoils and was implied in the paper by Chapman *et al.* In terms of $\widetilde{C}_p$, the distributions now compare as shown in Fig. 5b where the distance from the base is normalized by the distance to the reattachment point x_r. Except for the case with a long forebody, for which the boundary layer at separation, θ_s/h, is relatively large, there is fairly good collapse of the data. Govinda Ram and Arakeri [18] confirmed and extended such a plot. The apparent generality of the reattachment pressure rise gives hope that it might be worked into a wake model of incompressible base flow and that there may be a corresponding generalization for the supersonic case.

Several interesting features may be noted in Fig. 5b. Most prominent is the overall pressure-rise coefficient $\widetilde{C}_{pm} \doteq 0.35$. One may also estimate a value of the pressure coefficient at reattachment, $\widetilde{C}_{p_r} \doteq 0.27$; if the free shear layer were a canonical one (see Appendix) its value should be 0.32. Again, the question is whether there is dissipation of total pressure in the reattachment region or whether the experimental data are showing effects due to finite initial thickness, as indicated above for supersonic base flows.

4. FLOW OVER A STEP

This is the classical bluff-body problem for supersonic flow but is also being used widely for "validating" computational codes in incompressible flow. It represents perhaps the simplest separated flow. The so called "dead water" region (Fig. 6a) is enclosed by the two sides of the step and the zero streamline $\psi^* = 0$ which extends from the step shoulder to the reattachment point r. Since there is no mean outflow through the boundary, the momentum balance for the fluid inside it, "dead water" or not, is given by a balance of forces due to stresses on the boundary. The equation for this, first proposed by Sychev [6], is simply

$$p_b h + \int_0^{x_r} \tau^* \, dx = \int_0^h p^* \, dy$$

or

$$\int_0^h (p^* - p_b) \, dy = \int_0^{x_r} \tau^* \, dx \tag{1a}$$

Here, p^* and τ^* are the stresses on the zero streamline $\psi^* = 0$. For supersonic flow these are usually made non dimensional with the pressure p_1 but here we will put them in canonical form by referencing to $p_e = p_s = p_b$ or by the dynamic pressure $\frac{1}{2}\rho U_e^2$. The latter, valid also for

incompressible flow, gives

$$\int_0^h \widetilde{C}_{p^*}\, dy = \int_0^{x_r} C_{\tau^*}\, dx \tag{1b}$$

where $\widetilde{C}_{p^*} \equiv (p^* - p_b)/\frac{1}{2}\rho U_e^2$ is the canonical pressure coefficient introduced in the preceding section and $C_{\tau^*} \equiv \tau^*/\frac{1}{2}\rho U_e^2$ is the shear-stress coefficient for the mixing layer in terms of the velocity U_e at its outer edge, which will correspond to the velocity U_s on $\psi = 0$ from a free streamline model for the outer flow. Correspondingly the wake length L will be identified with $x_r = L$.

If further we define the mean values

$$\langle C_{\tau^*} \rangle \equiv \frac{1}{L} \int_0^{x_r} C_{\tau^*}\, dx \tag{2a}$$

and

$$[\widetilde{C}_{p^*}] = \frac{1}{h} \int_0^h \widetilde{C}_{p^*}\, dy \tag{2b}$$

the elements of the balance of stresses are simply exhibited in the equation

$$[\widetilde{C}_{p^*}]\, h = \langle C_{\tau^*} \rangle L$$

The length of the wake is given by

$$\frac{L}{h} = \frac{[\widetilde{C}_{p^*}]}{\langle C_{\tau^*} \rangle} \tag{3}$$

The problem is to determine suitable models for $[\widetilde{C}_{p^*}]$ and $\langle C_{\tau^*} \rangle$.

In modelling $[\widetilde{C}_{p^*}]$ it would be useful to incorporate into it the reattachment pressure C_{p_r}. This can be done by writing, instead of Eq. 2b, the alternative definition

$$\int_0^h \widetilde{C}_{p^*}\, dy \equiv \widetilde{C}_{p_r}\, h_e \tag{4}$$

where $h_e \equiv \kappa h$ is the equivalent height which, with $\widetilde{C}_{p_r}$, gives the upstream component of pressure force on $\psi^* = 0$. Thus $[\widetilde{C}_{p^*}] = (h_e/h)\, \widetilde{C}_{p_r} = \kappa \widetilde{C}_{p_r}$ and

$$\frac{L}{h} = \frac{\kappa \widetilde{C}_{p_r}}{\langle C_{\tau^*} \rangle} \tag{5}$$

Equations 3 and 5 display the fundamental parameters defining the base flow. *The normalized length or aspect ratio of the wake is determined by the balance between shear stress and pressure*

rise on the boundary streamline. The base pressure does not appear in this relation because it is implicit in the reduced pressure coefficient. In this model, the wake dynamics is universal, independent of the bluff-body geometry.

Ideally, for an asymptotic theory, cf the laminar problem [6], there would be a separation of scales: the free boundary would be at constant pressure everywhere except in a small region near r, at the end of the wake, in which the pressure rise would occur. However, turbulent mixing-layer spreading rates are finite and it is unlikely that the wakes of different bluff bodies have a universal description which is both simple and quantitatively accurate. With that precaution, we explore in this and following sections the implications of Eqs. (3) and (5), to try to obtain insights that are simple and still capture the essential dynamics.

Applying Eq. 3 or 5 to incompressible step flow (Fig. 6a) and using the canonical value $\langle C_{\tau^*} \rangle = 0.025$ gives $L/h = 40\,[C_{p^*}] = 40\,\kappa \widetilde{C}_{p_\tau}$. With a value for $\kappa = 0.65$, determined from the data of Arie and Rouse described in the next section, and with the canonical value $\widetilde{C}_{p_\tau} = 0.32$, the result is $L/h = 8.3$. This is considerably larger than typical values (6–7) found by various experimenters; it is not clear whether the laboratory values of $\langle C_{\tau^*} \rangle$ are higher than our "canonical" value or $\widetilde{C}_{p_\tau}$ is lower. For example, if $\widetilde{C}_{p_\tau} = 0.27$ is chosen from Fig. 5b then $L/h = 7.0$. This gives some indication of the sensitivity to actual conditions.

5. BLUFF-BODY FLOWS

The generalization of the step flow to a bluff-body flow, the flat plate with wake splitter, is shown in Fig. (6b). As before, there is a balance of forces on the fluid enclosed by the body and the zero streamlines. For convenience, we will refer to this region as the "bubble". On the upstream side of the bubble the pressure is p_b, ie, on that part next to the base of the body as well as on the zero streamline which separates from it. Pressure recovery occurs on the downstream side of the bubble. Thus the force-balance equation is similar to Eq (1) for the step, but with h now replaced by $H = \frac{1}{2}W$, the half width of the bubble:

$$\frac{L}{H} = \frac{[\widetilde{C}_{p^*}]}{\langle C_{\tau^*} \rangle} \tag{6a}$$

$$\text{or} \qquad \frac{L}{W} = \frac{1}{2}\,\frac{[\widetilde{C}_{p^*}]}{\langle C_{\tau^*} \rangle} = \frac{1}{2}\,\frac{\kappa \widetilde{C}_{p_\tau}}{\langle C_{\tau^*} \rangle} \tag{6b}$$

This is a universal relation for the aspect ratio of the wake bubble behind any bluff body, not only the flat plate. For the canonical values $\langle C_{\tau^*} \rangle = 0.025$, $\widetilde{C}_{p_\tau} = 0.32$ and with $\kappa = 0.65$, the relation gives $L/W = 4.2$, whereas with $\widetilde{C}_{p_\tau} = 0.27$ from Fig. 5b the result is $L/W = 3.5$.

Additional steps are needed to relate the bubble dimensions to the base pressure and body geometry. These are illustrated in Fig. 7 which has been constructed from the numerical solutions by Plesset and Shaffer [19] of the Riabouchinsky free-streamline model for wedges. Variation of the wedge half angle, $\frac{1}{2}\,\alpha_w$, from 0 (step flow) to 90° (flat plate) tracks a significant bluffness

parameter [15], namely the direction in which the separating streamline $\psi = 0$ leaves the body; eg. parallel to the free-stream direction for the step flow and perpendicular for the flat plate.

The closure is indicated in Fig. 7a which shows the dependence of base pressure C_{p_b} on wake aspect ratio L/W for several wedges and the flat plate. The intersection of L/W = const. with each curve determines a corresponding value of C_{p_b}. Then Fig. 7b can be used to determine values of L/d. The solutions for three choices of the wake parameter L/W (= 4.2 and 3.5, from above, and 3.1 from Table 2) are shown in Table 1.

	α_w degrees	30	60	90	180 (flat plate)
$\frac{L}{W} = 4.2$	C_{p_b}	-0.38	-0.45	-0.46	-0.47
	L/d	6.0	8.7	11	14
$\frac{L}{W} = 3.5$	C_{p_b}	-0.44	-0.52	-0.55	-0.56
	L/d		6.6	7.8	11
$\frac{L}{W} = 3.1$	C_{p_b}	-0.48	-0.58	-0.61	-0.63
	L/d		5.4	6.8	9.0

Table 1. Model data for wedges and flat plate, for three choices of L/W

For $\alpha_w \rightarrow 0$ the curves in Fig. 7 approach the axis $C_{p_b} = 0$; flow over a step corresponds to this limiting case and, within the context of this model, $C_{p_b} = 0$ for the incompressible step flow.

$\langle C_{\tau^*} \rangle = 0.028$

$[\widetilde{C}_{p^*}] = 0.24 \quad C_{p_r} = -0.02 \quad \widetilde{C}_{p_r} = 0.36 \quad \kappa = 0.65$

$L/W = 3.1$

$L/d = 8.4$

$C_{p_b} = -0.60$

Table 2. Experimental data for flat plate, obtained from Fig. 8 in Ref. 2.

The model results in Table 1 may be compared, in Table 2, with data from the measurements of Arie and Rouse [2] in the wake of a flat-plate bluff body with a splitter plate. In that unique experiment, measurements were obtained of the mean velocity field, the distribution of pressure C_p and of Reynolds stress $\overline{u'v'}$. From the velocity field they computed the streamlines, and modified the wind tunnel wall to correct for blockage effects. The results are presented in Fig. 8

of Ref. 2, which shows the computed streamlines and the profiles of u, C_p and $\overline{u'v'}$ at four locations, $x/L = 0.24, 0.48, 0.72$ and 0.96. Thus, although data for evaluating $[\widetilde{C}_{p^*}]$ and $\langle C_{\tau^*} \rangle$ are available at only four points on $\psi^* = 0$, these are the most complete set available. There may be some uncertainty in the values. For example, we obtained the value $\widetilde{C}_{p_r} = 0.36$ by extrapolation from the data at the four points; the data point at $x/L = 0.96$ was $\widetilde{C}_{p^*} = 0.32$, corrected from the measured value 0.26. Similarly from their hot-wire measurements of $(-\overline{u'v'})$ at four locations we determined the value $\langle C_{\tau^*} \rangle = 0.028$, somewhat higher than the canonical value 0.025. For this bluff-body configuration the conditions for a canonical free shear layer are favorable because the initial thickness θ_0/d of the shear-layer is very small after its acceleration on the face of the plate and because the pressure is constant over most of the free boundary, . The difficulty of measuring $\overline{u'v'}$ or the delicacy of the blockage corrections may account for the discrepancy, or it may be real.

The values, $\langle C_{\tau^*} \rangle = 0.028$ and $[\widetilde{C}_{p^*}] = 0.24$ listed in Table 2, give in Eq. 6b the wake aspect ratio $L/W = 4.3$ rather than the value 3.1 from the zero streamline pattern determined by Arie and Rouse (Fig. 2c). On the other hand, for $L/W = 3.1$ Riabouchinsky's free streamline model gives the values of C_{p_b} and L/d listed in Table 1 rather than those measured.

Thus the appropriate, "universal" value of L/W is uncertain. For the several values discussed, Fig. 7b and Table 1 show the corresponding changes of base pressure with change of the wedge angle. Corresponding values of drag coefficient for wedges with wake splitter can be found from the free-streamline model calculations [19]. With $L/W = 3.5$, they are $C_D = 0.49$, 0.79, 1.01 and 1.38 for $\alpha_w = 30, 60, 90$ and 180 deg., respectively.

6. THE SUPERSONIC CASE

As indicated in the Appendix, information about supersonic shear layers is much less complete than for the incompressible case. For one thing, the Mach number M_e at the edge of the layer is now an additional parameter. A strong effect of increasing M_e from zero is to reduce the growth rate of the shear layer $d\delta/dx$ and the magnitude of the shear stress coefficient C_{τ^*}, as indicated in Fig. A2. The change becomes slower for $M_e \gtrsim 2$; a value of $C_{\tau^*} \doteq 0.005$ may be a useful first estimate for values of $M_e > 2$, correspondingly for $M_1 \gtrsim 1.5$. While this is tentative, trying to obtain an estimate for $[\widetilde{C}_{p^*}]$ from available experimental data was even less rewarding. Pressure distributions on the reattachment wall are available but projecting them onto $\psi^* = 0$, accurately locating r and estimating $\widetilde{C}_{p_r}$ proved to be too uncertain.

Instead, to obtain some insights into $[\widetilde{C}_{p^*}]$, we work back from a known value of C_{p_b}, as follows. For $M_1 = 2.03$, Sirieix [14] obtained an asymptotic value $p_b/p_1 = 0.30$ by extrapolating experimental values to $\theta_s/h = 0$. This corresponds to $-C_{p_b} = 0.25$ and to a Prandtl-Meyer expansion which gives $L/h = 3.2$ (or $L/W = 1.6$) and $M_e = 2.80$. Thus, with $\langle C_{\tau^*} \rangle = 0.005$ in Eq. 3 a value for $[\widetilde{C}_{p^*}] \equiv \kappa \widetilde{C}_{p_r} = 0.016$ is obtained. This is considerably smaller than in the incompressible case but of course it has to balance a considerably smaller shear force. To see it in terms of $\kappa \widetilde{C}_{p_r}$ we estimate $\widetilde{C}_{p_r} = 0.2$ from pressure-distribution data in

Ref. 14. This gives $\kappa = 0.08$ compared to 0.65 for the incompressible case. In fact, one would expect κ to be considerably smaller in supersonic flow because the shear-layer spreading angle $d\delta/dx$ is smaller by a factor of 3 or 4 and because the shear layer approaches the reattachment point at a smaller angle.

For high values of M_1, the expansion from p_1 to p_b leads to even higher values of M_e, and it may be useful to examine the limiting case $M_e \gg 1$. The total pressure on $\psi^* = 0$ is given, for a perfect gas by $p_t^* = p_e\left(1 + \frac{\gamma-1}{2} M^{*2}\right)^{\frac{\gamma}{\gamma-1}}$, where $M^* = u^*/a^*$. Now $u^* = cU_e$, where c is some constant for that limiting case; to obtain a^* we assume the adiabatic relation $a^{*2} = a_e^2 + \frac{\gamma-1}{2}\left(U_e^2 - u^{*2}\right) \sim \frac{\gamma-1}{2} u^{*2}\left(\frac{1}{c^2} - 1\right)$, for $a_e \ll U_e$. Then $p_t^*/p_e = \left(1 - c^2\right)^{\frac{\gamma}{\gamma-1}} \equiv \chi$ is a finite limiting value. From the basic equation (1a) and assuming $p_r = p_t^*$, one then obtains

$$\frac{L}{h} \sim \frac{\kappa(\chi - 1)}{\langle \tau^* \rangle / p_e} = \frac{\kappa(\chi - 1)}{\frac{1}{2}\gamma M_e^2 C_{\tau^*}}$$

It is noted in the Appendix that C_{τ^*} and $d\delta/dx$ (thus κ) decrease (slowly) with increasing $M_e \gtrsim 2$. If C_{τ^*}/κ has a limiting value or decreases more slowly than M_e^2, as seems likely, then L/h decreases with increasing M_e, and this agrees with the observed trend (eg. Refs. 13, 14). All this is rather speculative and it suggests that there are still interesting problems to be settled for compressible turbulent shear layers.

7. CONCLUDING REMARKS

The preceding outlines an attempt to model the base pressure of bluff bodies, in supersonic and incompressible flow, by working with the balance of stress forces on the mean near wake defined by the closure streamline $\psi^* = 0$. By referencing the stress coefficients to the base pressure and the corresponding dynamic pressure $\frac{1}{2}\rho U_e^2$, the near wake dynamics is uncoupled from the overall flow, even for the incompressible case, and is seen to be determined by the fundamental parameters $\langle C_{\tau^*} \rangle$, $[\widetilde{C}_{p^*}]$ and L/W. The wake aspect ratio L/W is established by the balance between the shear-stress force $\langle C_{\tau^*} \rangle$ and the pressure-rise force $[\widetilde{C}_{p^*}]$. As it stands, the accuracy of the model is not high, but it may provide a framework which displays the fundamental dynamics of the problem and on which improvements can rationally be made. For example, with the role of the shear-layer stress displayed, the effects of parameters such as Reynolds number, initial shear-layer thickness, external perturbation, etc. that affect the shear stress can be rationally incorporated.

For the incompressible case, the reduced coefficients $\langle C_{\tau^*} \rangle$ and $[\widetilde{C}_{p^*}]$ are assumed to have universal values for the "asymptotic" condition $\theta_s/h \to 0$; this leads to the conclusion that L/W has a universal value $L/W(\sim 3.5)$ for all bluff bodies with wakes stabilized against vortex shedding. The connection to a particular bluff body is then made through a free-streamline model for that body and this determines C_{p_b} as well as L/d and W/d. Numerical estimates of the parameters, given in Table 1 for incompressible flow, indicate the sensitivity to those values. A model of a reattaching shear layer would be helpful for improving the evaluation of $[\widetilde{C}_{p^*}]$, as

well as $\langle C_{\tau^*} \rangle$. The free-streamline model also introduces some uncertainty; a different model (e.g. the "re-entrant jet" model) will give a slightly different dependence of the wake geometry on C_{p_b}.

For the supersonic case the limitations are more serious. Information is still needed about the structure of turbulent shear layers (τ^*, u^*, p_t^*) at high Mach number. It is ironical that, following the line of thought described in previous sections, we are unable to complete the picture quantitatively for supersonic base flow because of insufficient information about supersonic reattachment pressure rise, with which the Chapman-Korst criterion dealt (apparently) so efficiently!

APPENDIX: TURBULENT FREE SHEAR LAYERS

The state of the shear layer which forms the free boundary of the base flow is crucial in the dynamics of that flow. The state depends on many factors, and usually cannot be described simply, but it will be useful for reference to summarize here the properties of canonical turbulent free shear layers, i.e. those that have developed at sufficiently high Reynolds number and sufficiently far from initial conditions tc have reached an equilibrium turbulent structure with self similar mean values, in particular, a mean velocity profile $u = U_e F(\eta)$ and shear stress distribution $\tau = \tau_m g(\eta)$ where $\eta \equiv y/x$. The growth rate of the layer $d\delta/dx \equiv \delta' = \text{const.}$ The momentum integral can be used to find the self similar shear stress $\tau(\eta)$ for a measured velocity profile $u(\eta)$. In particular, the shear stress τ^* on $\psi^* = 0$, which is in fact the maximum stress, can be found from the momentum integral:

$$\tau^* = \tau_m = \frac{d}{dx} \int_{y^*}^{\infty} \rho u \, (U_e - u) \, dy = \frac{d}{dx} \int_{-\infty}^{y^*} \rho u \, (u - U_i) \, dy$$

Here, the unique ray $y^* = \eta^* x$ coincides with the zero streamline $\psi^* = 0$ which has its origin at the separation point ($x = 0$, $y = 0$); U_e and U_i are the free-stream velocities on either side (but for the base-flow modelling we take $U_i = 0$). The equality of integrals in this equation can be used to calculate η^*. Then the velocity on the dividing streamline, $u^* = u(\eta^*)$ can be determined. This, in effect, was the procedure used by Chapman and by Korst, who were particularly interested in u^*, correspondingly M^* and p_t^*. Here we are interested in also making use of τ^*. Other quantities that may be of interest are the displacement thicknesses of the flow above and below $\psi^* = 0$. These may be expressed as the positive displacement wedge angle above $\psi^* = 0$,

$$\frac{d\delta_+^*}{dx} = \int_{\eta^*}^{\infty} \frac{\rho}{\rho_e} \left(1 - \frac{u}{U_e} \right) d\eta$$

and the negative displacement thickness or equivalent entrainment angle below $\psi^* = 0$,

$$\frac{d\delta^*_-}{dx} = \int_{-\infty}^{\eta^*} \frac{\rho}{\rho_e}\left(\frac{u}{U_e} - \frac{U_i}{U_e}\right) d\eta$$

For *incompressible* flow with $U_i = 0$, we believe that the best defined self similar mixing layer is the one measured by Liepmann and Laufer [20]. The following "canonical" values have been calculated for their velocity profile:

$$u^*/U_e = 0.57\,, \quad \text{thus} \quad C_{p_t^*} = (0.57)^2 = 0.32$$

$$\tau^*/\tfrac{1}{2}\rho U_e^2 \equiv C_{\tau^*} = 0.025$$

$$d\delta^*_+/dx = 0.020$$

$$d\delta^*_-/dx = 0.034$$

For *supersonic* shear layers, these quantities depend on M_e, ρ_i/ρ_e, γ, and are not as well defined as for the incompressible case. Very few measurements exist for demonstrated canonical conditions, which are more difficult to achieve experimentally at supersonic conditions.

From Chapman's and from Korst's results one can work back to the values of total pressure p_t^* and $C_{p_t^*}$ that they calculated. These are shown in Fig. A1, from Ref. 21. The laminar case (Chapman) was computed from exact equations but the turbulent case (Korst) is subject to the uncertainties of turbulence modelling. For example, it gave for $M_e = 0$ the value $C_{p_t^*} = 0.38$ rather the value 0.32 based on the data of Ref. 20.

For the turbulent shear stress C_{τ^*}, the most relevant data appear to be those of Elliott and Samimy [22], who determined values of τ_m from measured velocity profiles and also measured Reynolds stresses directly. Their data provide values of $\tau_m/\rho(U_e - U_i)^2$ for free shear layers with $(M_e,\, M_i) = (1.80,\, 0.51)$, $(1.97,\, 0.37)$ and $(3.0,\, 0.45)$, corresponding to convective Mach numbers $M_c = 0.51,\ 0.64$ and 0.86, respectively. They are plotted in Fig. A2 against M_e, for $M_i = 0$, by using the "convective Mach number" concept [23] to make the correspondence with M_c. The somewhat arbitrary curve joins these points to the canonical value $C_{\tau_m} = 0.025$ at $M_c = 0$; it exhibits a rapid decrease with increasing compressibility, M_c, similar to that which has been observed for the growth rate $d\delta/dx$, but which tends to decrease more slowly at $M_c > 1$. Again, accuracy of the numbers resulting from our adaptations is uncertain.

Finally, note must be made of the effects, on the magnitudes of these quantities, of departures from asymptotic, equilibrium conditions in the free shear layers which exist in actual base flows. In particular, the effects of initial conditions at separation, usually expressed in terms of the boundary-layer momentum thickness θ_0, delay the attainment of equilibrium conditions on ψ^*. Bradshaw [24] found, in subsonic mixing layers, that the distance x along the shear layer to reach equilibrium was 500 to 1,000 θ_0, whether the initial boundary layer was laminar or turbulent. For laminar initial conditions, transition occurs soon after separation and $\tau_m(x)$ overshoots the final equilibrium value, but for turbulent separation, $\tau_m(x)$ approaches the equilibrium value from below. In a base flow, with $x_r \sim 6h$, say, and $\theta_0/h = 0.01$, the wake length $x_r/\theta_0 = 600$, which is near the lower limit of Bradshaw's criterion. Thus the average value of shear stress on the base-flow boundary $\langle C_{\tau^*} \rangle$ will be lower than the equilibrium value for turbulent boundary-

layer separation, but may be higher if there is laminar separation followed by transition. As function of θ_0/h, the wake length will be shortest and the base drag highest in the transition region, where $\langle C_{\tau *} \rangle$ will have its maximum value.

ACKNOWLEDGMENTS

Ideas in this paper developed from research supported over many years by the Office of Naval Research, U.S. Navy, most recently under Grant No. N00014-94-1-0793. F. Noca and S. Valluri assisted in preparation of the figures.

REFERENCES

[1] Kirchhoff, G. 1869 Zur Theorie freier Flüssigkeitsstrahlen **Crelle 70**, 416.

[2] Arie, M. and Rouse, H. 1956 Experiments on two-dimensional flow over a normal wall. *J. Fluid Mech.* **1**, 129-141.

[3] Fage, A. and Johansen, F.C. 1927 On the flow of air behind an inclined flat plate of infinite span. *Proc. Roy. Soc.* **A 116**, 170–197.

[4] Riabouchinsky, D. 1920 On steady fluid motion with free surfaces. *Proc. London Math. Soc. Ser. 2*, **19**, 206–215.

[5] Roshko, A. 1993 Perspectives on Bluff Body Aerodynamics. *J. Wind Engineering and Industrial Aerodynamics* **49**, 79–100.

[6] Sychev, V. V. 1982 Asymptotic theory of separated flows. *Mekh. Zhidkosti i Gaza* No. 2, 20–30.

[7] Chapman, D.R., Kuehn, D.M., and Larson, H.K. 1957 Investigation of separated flows in supersonic and subsonic streams with emphasis on the effect of transition. NACA Rept. 1356; also NACA RM A55L14, 1956.

[8] Korst, H.H. 1956 A theory for base pressures in transonic and supersonic flow. *J. Appl. Mech.* **23**, 593–600.

[9] Hama, F.R. 1968 Experimental studies on the lip shock. *AIAA J.* **6**, 212–219.

[10] Tanner, M. 1970 Druckverteilungs messungen an Keilen bei Kompressibler Strömung. *Z. Flugwiss* **18**, 202–208.

[11] Nash, J.F. 1963 An analysis of two-dimensional base flow including the effect of the approaching boundary layer. Aeronaut. Res. Council R&M No. 3344.

[12] Chapman, D.R. and Korst, H.H. 1957 Theory for base pressures in transonic and supersonic flow. Correspondence in *J. Appl. Mech.* **24**, 484–485.

[13] Sirieix, M., Mirande, J. and Delery, J. 1966 Experiences fondamentales sur le recollement turbulent d'un jet supersonique. In: *Separated Flows*, AGARD CP No. 4, 353–392.

[14] Sirieix, M. 1960 Pression de culot et processus de mélange turbulent en écoulement supersonique plan. La Recherche Aéronautique No. 78, 13–22.

[15] Tanner, M. 1973 Theoretical prediction of the base pressure for steady flow. *Prog. in Aero. Sci.* **14**, 177–225.

[16] Roshko, A. and Lau, J.C. 1965 Some observations on transition and reattachment of a free shear layer in incompressible flow. *Proc. Heat Transfer and Fluid Mechanics Institute*, University of California at Los Angeles, A.F. Charwat (Ed.)

[17] Crabtree, L.F. 1957 Effects of leading-edge separation on thin wings in two-dimensional incompressible flow. *J. Aeronaut. Sci.* **24**, 597.

[18] Govinda Ram, H.S. and Arakeri, V. 1990 Studies on unsteady pressure fields in the region of separating and reattaching flows. *Trans. ASME J. Fl. Engg.* **112**, 402–408.

[19] Plesset, M.S. and Shaffer, P.A., Jr. 1948 Cavity drag in two and three dimensions. *J. Appl. Phys.* **19**, 934–939.

[20] Liepmann, H.W. and Laufer, J. 1947 Investigations of free turbulent mixing. NACA TN 1257.

[21] Roshko, A. and Thomke, G.J. 1966 Observations of turbulent reattachment behind an axisymmetric downstream-facing step in supersonic flow. *AIAA J.* **4**, 975–980 and Douglas Rept. SM-43069 (1965).

[22] Elliott, G.S. and Samimy, M. 1990 Compressibility effects in shear layers. *Phys. Fluids A* **2**, 1231–1240.

[23] Papamoschou, D. and Roshko, A. 1988 The compressible turbulent shear layer: an experimental study. *J. Fluid Mech.* **197**, 453–478.

[24] Bradshaw, P. 1966 The effect of initial conditions on the development of a free shear layer J. Fluid Mech. **26**, 225–236.

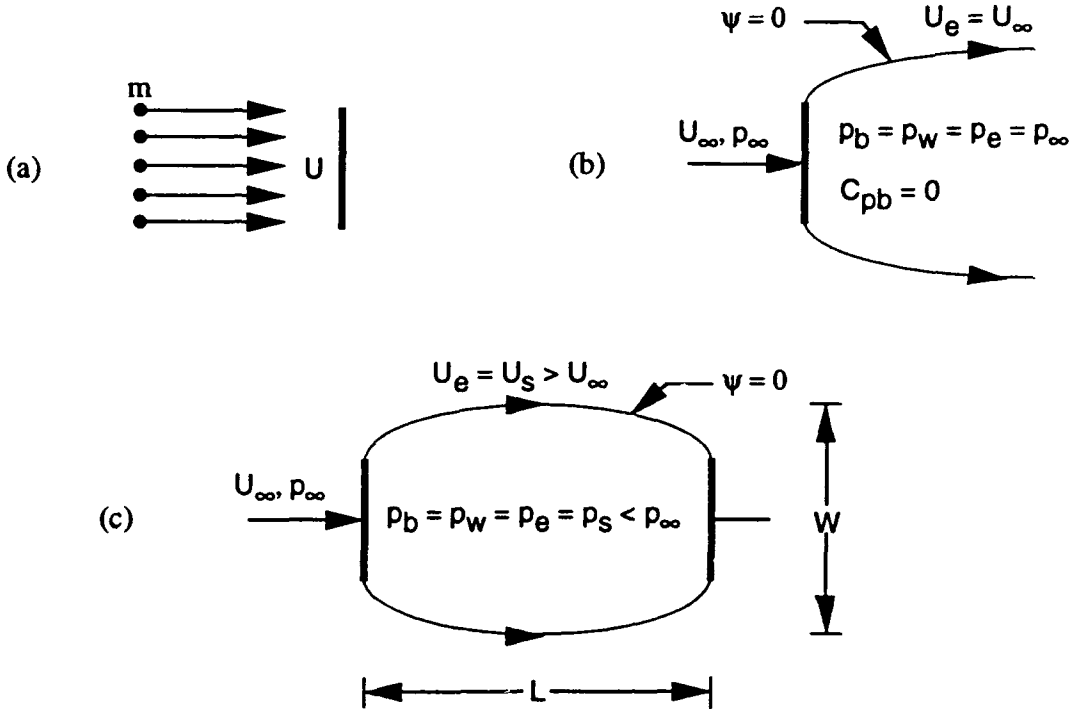

Figure 1. Bluff body models. (a) Newton's particle flow;
(b) Kirchhoff's free-streamline flow with $C_{p_b} = 0$;
(c) Riabouchinsky's free-streamline flow with arbitrary $C_{p_b} < 0$.

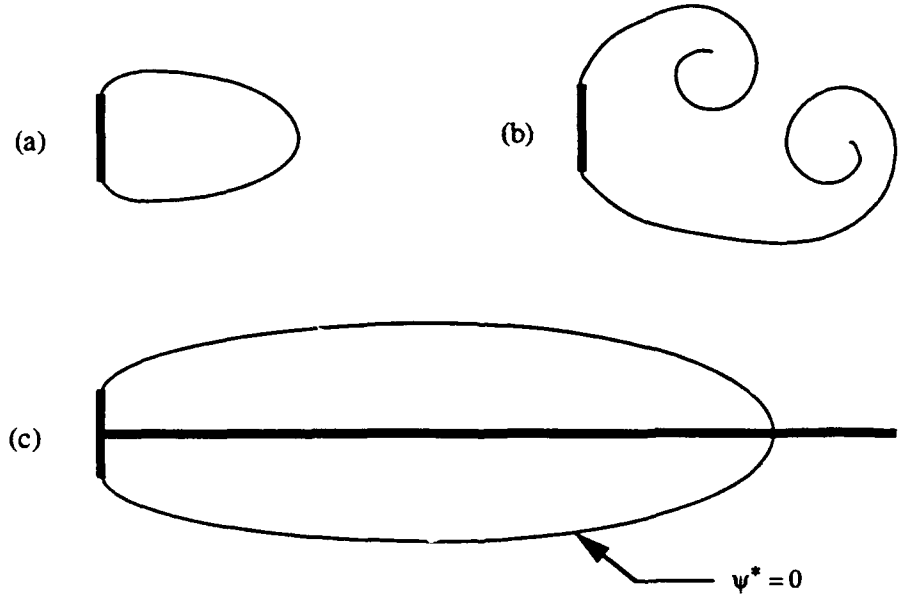

Figure 2. Wake of flat plate. (a) Mean flow [2];
(b) Corresponding instantaneous vortex-shedding flow;
(c) Mean flow with splitter plate [2].

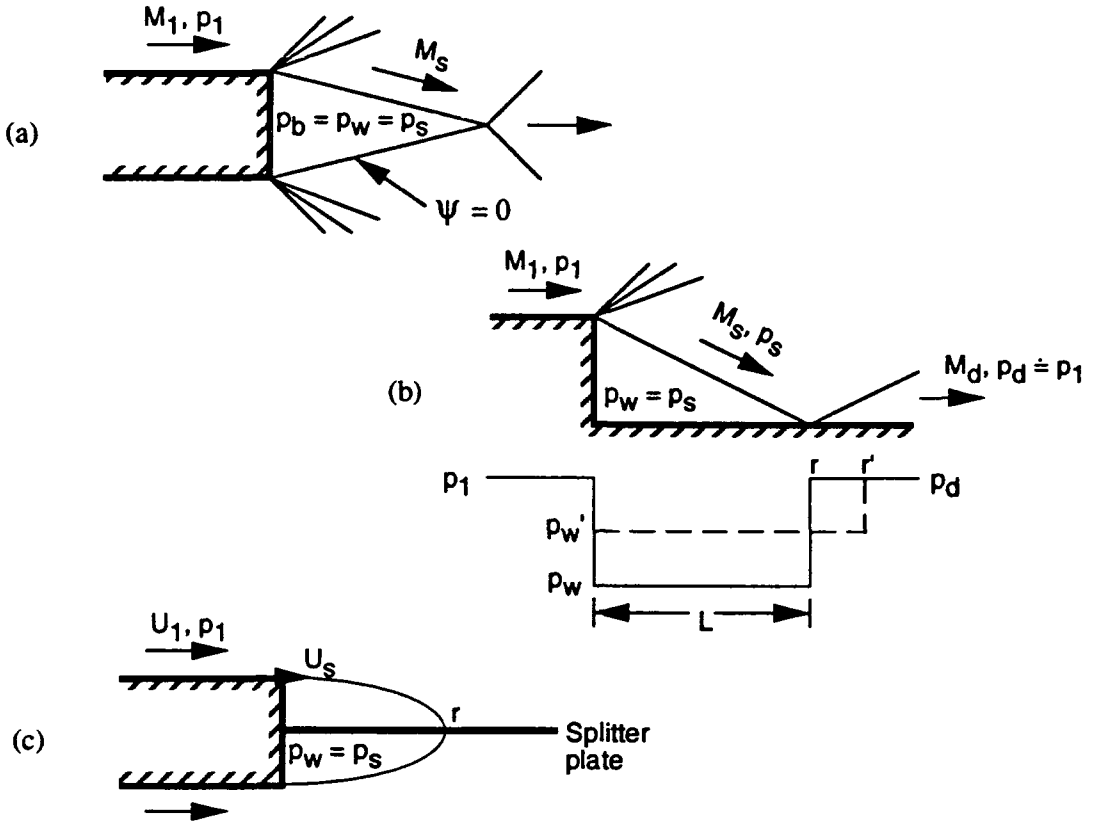

Figure 3. Free-streamline representations of flows over bases and steps. (a) Supersonic base flow; (b) Supersonic flow over a step; (c) Subsonic base flow with splitter plate.

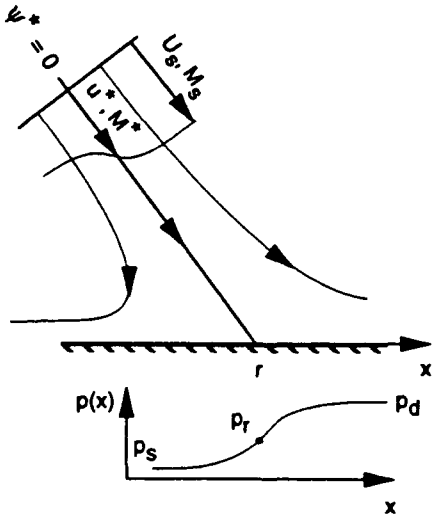

Figure 4. Sketch of reattaching free shear layer and pressure rise.

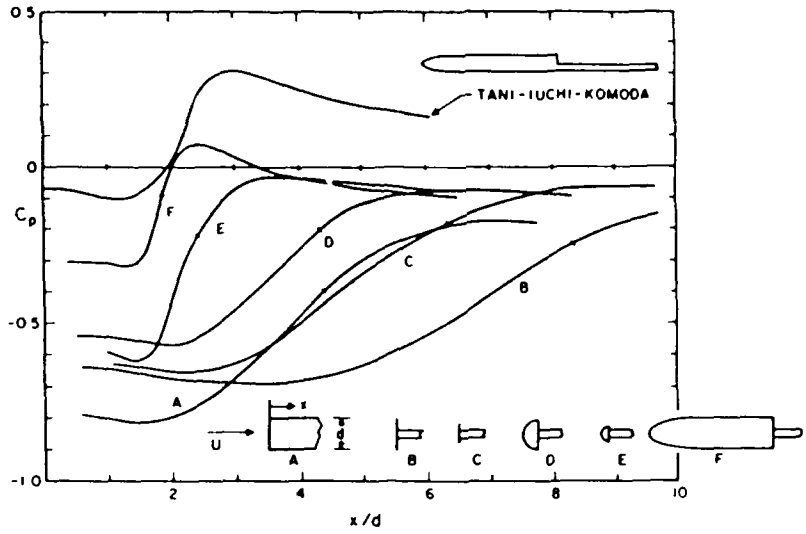

(a)

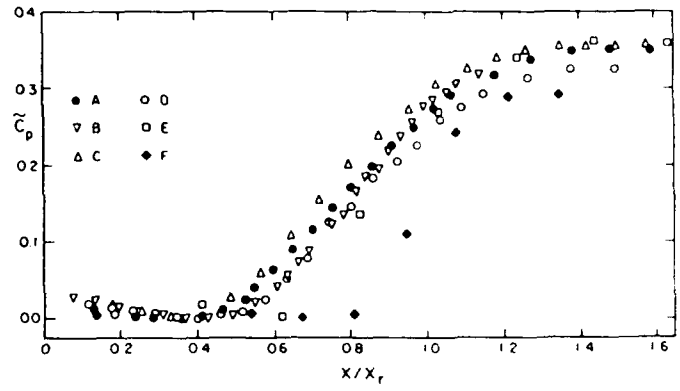

(b)

Figure 5. Reattachment Pressure Distributions [16]. (a) Conventional pressure coefficient. Reattachment point marked by cross-bar. (b) Reduced pressure coefficient.

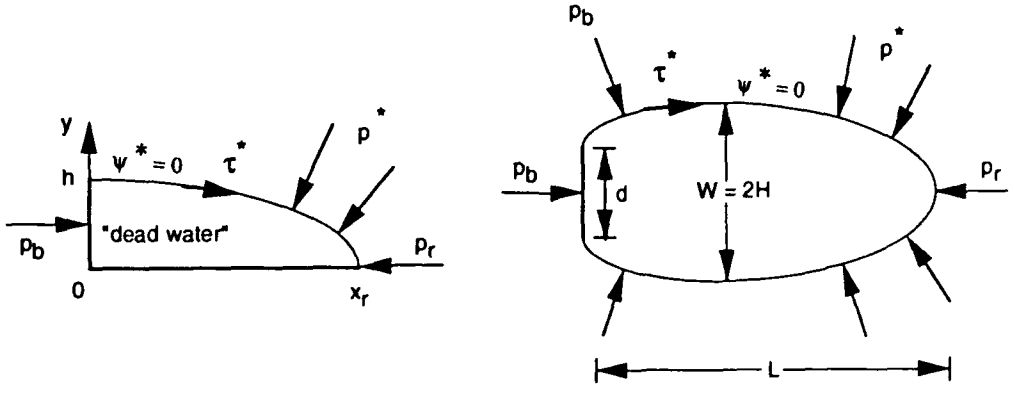

(a) (b)

Figure 6. Balance of shear-stress and pressure forces on the boundary enclosing the mean near wake. (a) Base flow past a step; (b) Wake of a flat plate.

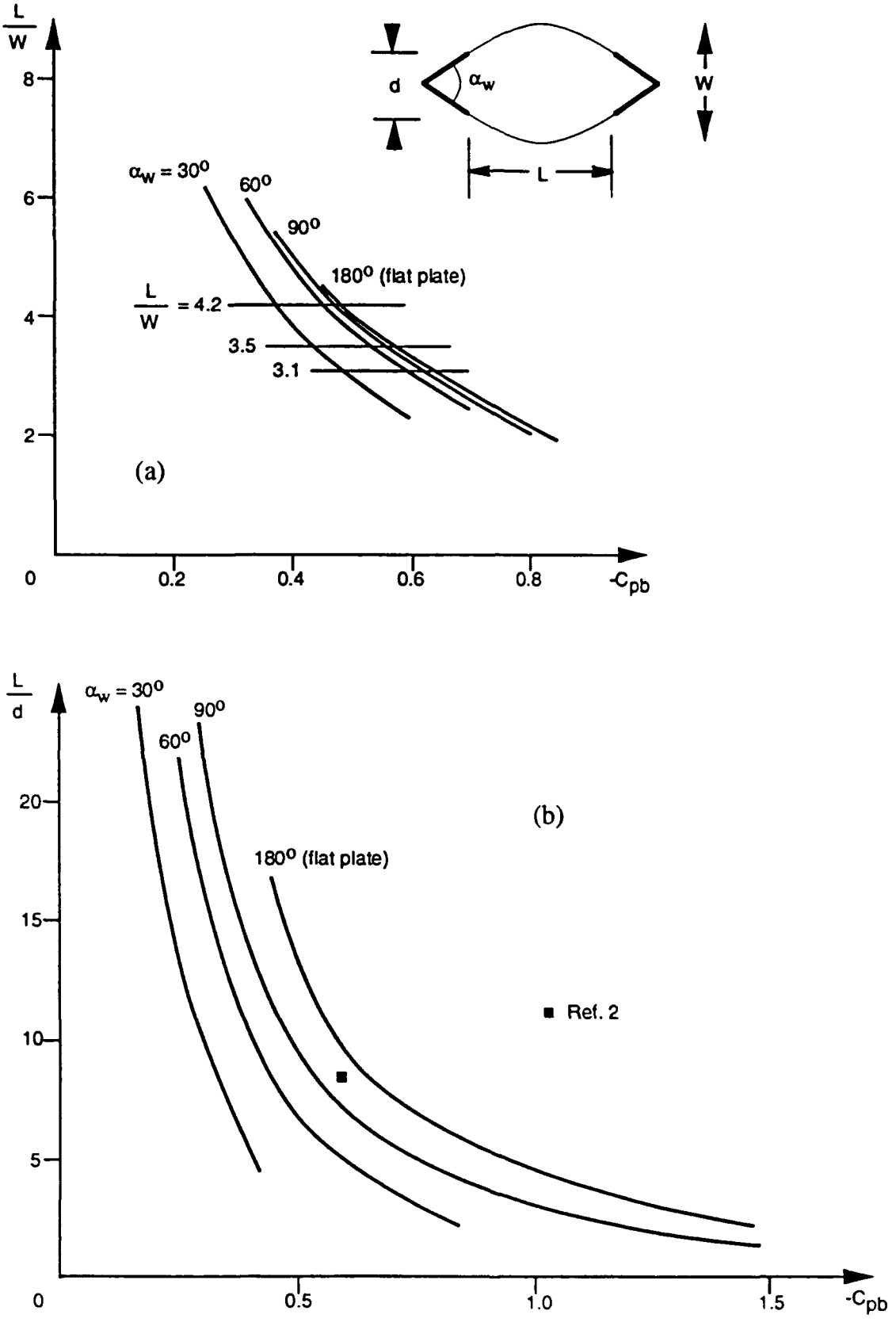

Figure 7. Wake parameters for bluff wedges and the flat plate.
(a) Wake aspect ratio; (b) Wake length. [19]

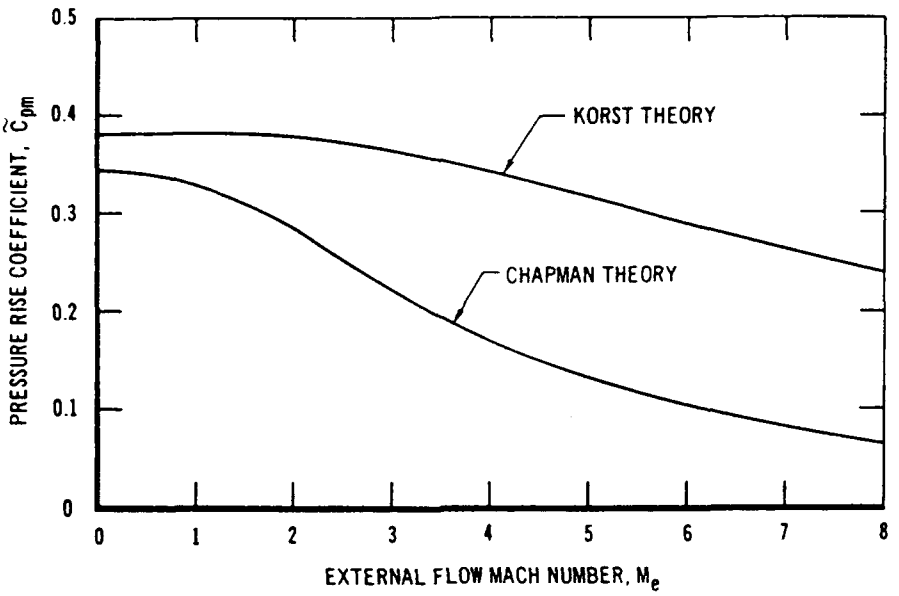

Figure A1. Canonical pressure rise coefficient ($\tilde{C}_{pm} = C_{p_t^*}$) for laminar (Chapman) and turbulent (Korst) free shear layers (from Ref. 21).

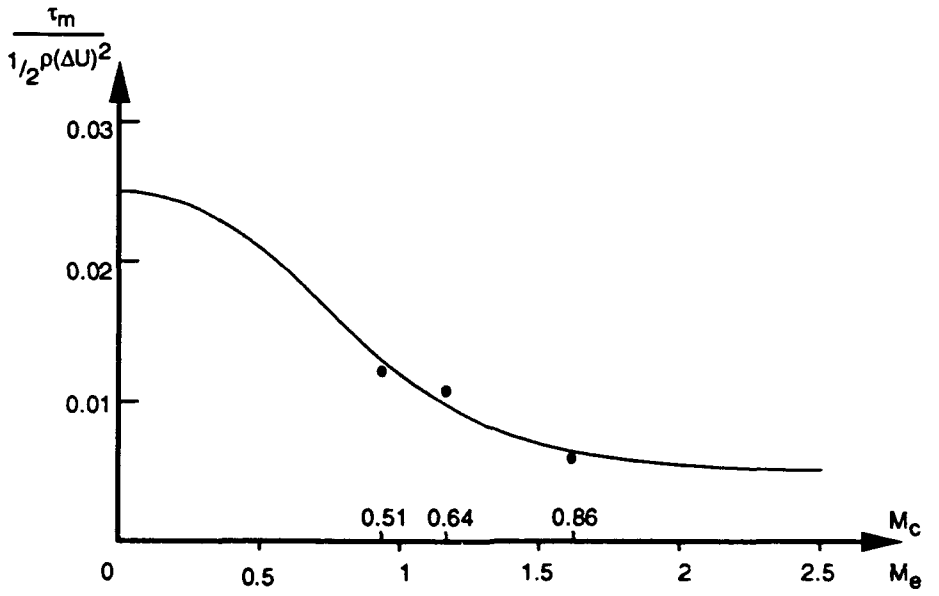

Figure A2. Maximum shear stress in compressible mixing layer. Data of Elliot and Samimy [22] compared with the canonical incompressible value $\tau_m/\left(\frac{1}{2}\rho\Delta U^2\right) = 0.025$.
(M_e scale is for $M_i = 0$)